ELSEVIER

Polymer 41 (2000) 7667–7679

polymer

Crystallization behaviour of poly(*N*-methyldodecano-12-lactam) Part 2. Recrystallization

J. Kratochvíl*, A. Sikora, J. Baldrian, J. Dybal, R. Puffr

Institute of Macromolecular Chemistry, Academy of Sciences of the Czech Republic, 162 06 Prague 6, Czech Republic

Received 4 June 1999; received in revised form 20 January 2000; accepted 7 February 2000

Abstract

The recrystallization process of poly(*N*-methyldodecano-12-lactam) MPA has been studied by differential scanning calorimetry (DSC), wide- and small-angle X-ray scattering (WAXS, SAXS) and Raman spectroscopy. During this irreversible process, the primary crystalline structure with a melting temperature of about 324 K is transformed to the higher-ordered final structure melting at 335 K. Isothermal recrystallization has an optimum at 327–329 K. During recrystallization, no change in crystalline modification takes place; however, crystallinity is increased from 30 to 35% (by WAXS) and the long period rises from 10.0 to 11.2 nm. The MPA sample recrystallized at 327 K and relaxed at laboratory temperature shows the melting point of 338.8 K. Crystallization/recrystallization of MPA is a diffusion-controlled kinetic process dependent on molecular weight and the rate of temperature changes. On the molecular level, the crystallization/recrystallization processes taking place in MPA can be interpreted as being directed by two conformational transitions in MPA molecules, namely the *trans*/*cis* transition on the C–N bond and the *gauche*/*trans* transition of the C–C sequences.

Keywords: *N*-methylated polyamide; Differential scanning calorimetry; Recrystallization

1. Introduction

Poly(*N*-methyldodecano-12-lactam) MPA shows a complex crystallization/melting behaviour [1–4]. Multiple-endotherm/exotherm DSC thermograms are often interpreted as a record of primary crystallization, secondary crystallization and recrystallization of a polymer system [5,6]. Recrystallization can also be accounted for as a transition between different polymorphic forms [7,8] or as a perfection step between non-integral and integral folded crystals [9]. A combination of coexistence of two types of crystalline structures with subsequent recrystallization was also studied [10].

In the first part of this study [1], the DSC, WAXS and Raman methods have shown a complex melting/crystallization behaviour of the MPA samples crystallized isothermally at different temperatures in the temperature range from 250 to 305 K. Multiple-peak DSC thermograms are interpreted as a stepwise process. During isothermal crystallization at greater supercoolings (crystallization temperature 250–280 K), a relatively well ordered structure is formed as primary lamellae showing the melting endotherm at about 324 K. During the later stages of isothermal crystallization in the given interval, less ordered "fringed" lamellae are formed. These crystallites are associated with the so-called secondary crystallization and their melting temperature strongly depends on the crystallization temperature. As the system is heated during the DSC run, a pronounced exotherm occurs at about 300 K that is associated with additional crystallization of the ordered structure (endotherm at 324 K). At the crystallization temperatures 290 K and higher, these two stages combine in a single isothermal crystallization step. On further heating during the DSC scan, the system undergoes a recrystallization process associated with an exotherm at about 326 K. A more perfect final crystalline structure thus formed melts at about 336 K. This highest melting endotherm shows a negligible dependence on crystallization temperature. Within 24 h at 300 K the MPA sample ($M_w = 14\,900$) reaches the crystallinity of about 34%.

This second part of the study provides a deeper insight into the phenomenon of recrystallization of MPA and a more thorough elucidation of crystallization/melting processes taking place in the system.

* Corresponding author.
E-mail address: jakr@imc.cas.cz (J. Kratochvíl).

0032-3861/00/$ - see front matter
PII: S0032-3861(00)00146-4

2. Materials and methods

Three samples of poly(*N*-methyldodecano-12-lactam) MPA used in this study were prepared by acidolytic polymerization of *N*-methyldodecano-12-lactam [11] followed by extraction with diethyl ether and final drying at 45°C. The samples, designated as MPA 5, MPA 15 and MPA 45 have the weight-average molecular weight (by light scattering) 4500, 14 900, and 46 700, respectively. (For more details on the samples see the first part of this study [1].)

A Perkin–Elmer DSC 2 apparatus was employed for calorimetric studies. The general procedure is described in detail elsewhere [1]. In the recrystallization studies, the as-prepared samples of MPA in the DSC pans were heated (heating rate, HR, 320 K/min) to respective annealing temperatures T_a in the range 320–331 K, kept there for 20 min, cooled down (cooling rate, CR, −10 K/min) to 300 K and scanned at HR = 10 K/min.

In the studies of influence of the cooling rate on crystallization of MPA, the samples were melted (360 K, 10 min), cooled down at different CR (−1.25 to −320 K/min) to 230 K and DSC scans were immediately recorded at HR = 10 K/min.

For small-angle X-ray scattering (SAXS) measurements, a Kratky diffractometer (A. Paar, Austria) coupled with a one-dimensional position-sensitive detector (JINR Dubna, Russia) was used. The CuKα radiation filtered electronically and with a Ni filter was used. SAXS curves were desmeared and Lorentz-corrected. Peak positions of SAXS reflections were employed to obtain long periods (LP) from Bragg's law, $L = 2\pi/q$, ($q = (4\pi/\lambda)\sin\theta$, where λ is the X-ray wavelength and 2θ is the diffraction angle). WAXS measurements are described elsewhere [1].

The apparatus and the method used in the Raman spectroscopic measurements are described elsewhere [1]. In recrystallization studies, the samples were heated under vacuum at 327 K for 20 min, cooled down to room temperature and measured.

3. Results and discussion

Throughout the text below, the same designation of respective endotherms and exotherms in the DSC thermograms of MPA is used as in the first part of this study. The reader is, therefore, referred to Fig. 1 of the first part [1].

3.1. Recrystallization

Recrystallization on melting is a characteristic feature of MPA. In the DSC thermograms, it is associated with the recrystallization exotherm E III appearing at about 326 K [1]. In the samples of higher molecular weight, particularly MPA 45, the recrystallization process is slower and, consequently, the recrystallization exotherm is less pronounced, which is probably associated with a low mobility of longer polymer chains. In this part of the study, the recrystallization process of MPA has been subjected to a more thorough investigation, the main aim of which being to find an optimum recrystallization temperature and to provide a possible explanation of the phenomena taking place during complex melting/crystallization/recrystallization behaviour of MPA.

In these experiments the as-prepared samples of MPA were annealed at different temperatures in the range of 320–331 K for 20 min. The respective thermograms of MPA 5 are shown in Fig. 1. Here, the thermogram of 318 K corresponds to the original as-prepared sample. The sample is partially recrystallized with the still prevailing less-ordered lamellar structure III showing the melting endotherm at about 326 K. With rising annealing temperature T_a the endotherm of structure III decreases and its maximum shifts towards higher temperatures. At $T_a = 322$ and 325 K structure III is exhibited only as a hump on the low-temperature branch of endotherm IV. At $T_a = 327$ and 329 K endotherm III is barely detectable and recrystallization to structure IV is almost complete.

At $T_a = 331$ K, which is obviously beyond the recrystallization optimum and also higher than the melting temperature of structure III in the as-prepared sample, endotherm III again appears and, moreover, a distinct endotherm at 321 K, i.e. below the T_a, is found which is also slightly apparent in the thermograms for $T_a = 327$ and 329 K. During annealing at 331 K structure III of the as-prepared sample melts and partially recrystallizes to structure IV. But a considerable part of it remains in the amorphous melt where imperfect "fringed" lamellae of structure II are formed during cooling (CR = −10 K/min) to 300 K before the DSC scan.

Moreover, in the thermogram of the as-prepared sample (318 K) another higher-melting endotherm at about 340 K appears on the descending branch of endotherm IV. In the thermogram for $T_a = 320$ K this high-melting endotherm is less apparent and at higher T_a it vanishes. There is no evidence of the origin of this endotherm. A possible explanation might be fractional crystallization of higher-molecular-weight portions of MPA during prolonged storage of the as-prepared sample at laboratory temperature.

The thermograms obtained with the samples of MPA 15 and MPA 45 annealed at 318, 327 and 331 K are shown in Fig. 2. After annealing at $T_a = 318$ K (as-prepared samples), the recrystallization is exhibited as a hump on the descending branch of endotherm III. At $T_a = 327$ K the resulting thermograms of MPA 15 and MPA 45 are quite similar to that of MPA 5 which implies that even in the higher-molecular-weight samples recrystallization is almost complete after annealing for 20 min at this temperature. During annealing at 331 K the melted structure III is to a lesser extent transformed to the higher-ordered structure IV. On the other hand, more "fringed" lamellae II melting on rescanning at about 322 K are formed on cooling to 300 K.

From the thermograms in Figs. 1 and 2 it is evident that in the MPA system an equilibrium exists under given conditions between the lamellar structures III and IV. The ratio of

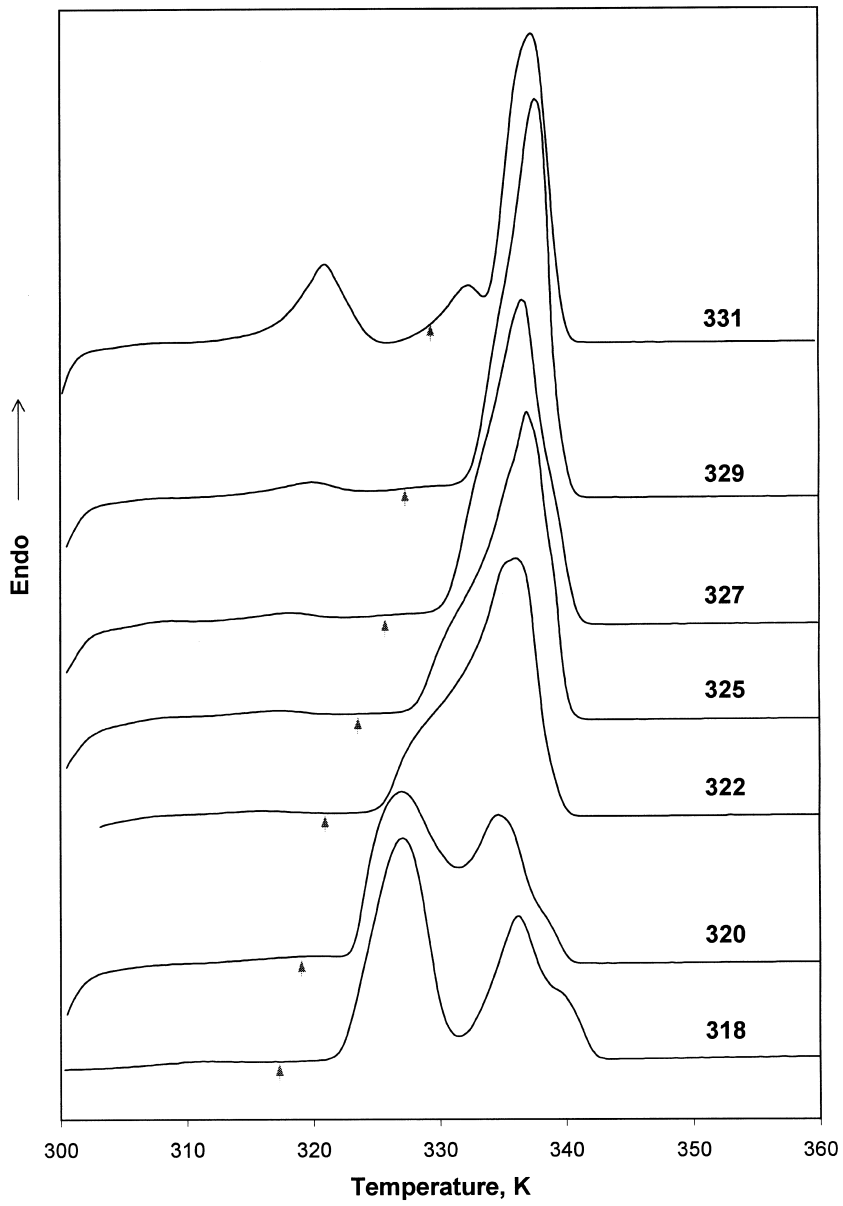

Fig. 1. The DSC thermograms of MPA 5 annealed at indicated temperatures T_a (K) for 20 min, cooled (CR = −10 K/min) to 300 K and scanned (HR = 10 K/min). The arrows indicate respective T_a.

these structures is a function of temperature and the kinetics of the III/IV transition is influenced by molecular weight.

The thermograms in Figs. 1 and 2 were evaluated quantitatively from the viewpoint of the overall enthalpic balance. The results are summarized in Fig. 3. The resulting values correspond to crystallinity of the MPA samples after annealing at the respective T_a.

In the case of the MPA 5 samples crystallinity shows a flat maximum at about 322–325 K; with increasing T_a crystallinity decreases and after annealing at $T_a = 331$ K, it reaches approximately the same value as that of the as-prepared sample. It can be seen that in the low-molecular-weight sample the processes of recrystallization from III to IV and the subsequent formation of II during cooling are relatively fast.

In the case of the MPA 15 and MPA 45 samples, there might be a maximum of crystallinity in the interval of 318–327 K, but after annealing at 331 K, crystallinity of the samples drops dramatically. Obviously, during annealing beyond the recrystallization optimum, the melted structure III of the higher-molecular-weight samples is transformed to the more perfect structure IV to a lesser degree and, after crystallization of the "fringed" lamellae II on cooling, a substantial portion of the polymer remains in the amorphous state which results in a markedly lower overall crystallinity as compared with the as-prepared samples.

In searching for the temperature optimum of recrystallization, an attempt was made at deconvoluting peaks III and IV in Fig. 1. Clearly, this procedure is semiquantitative only and subject to a high degree of arbitrariness. It can,

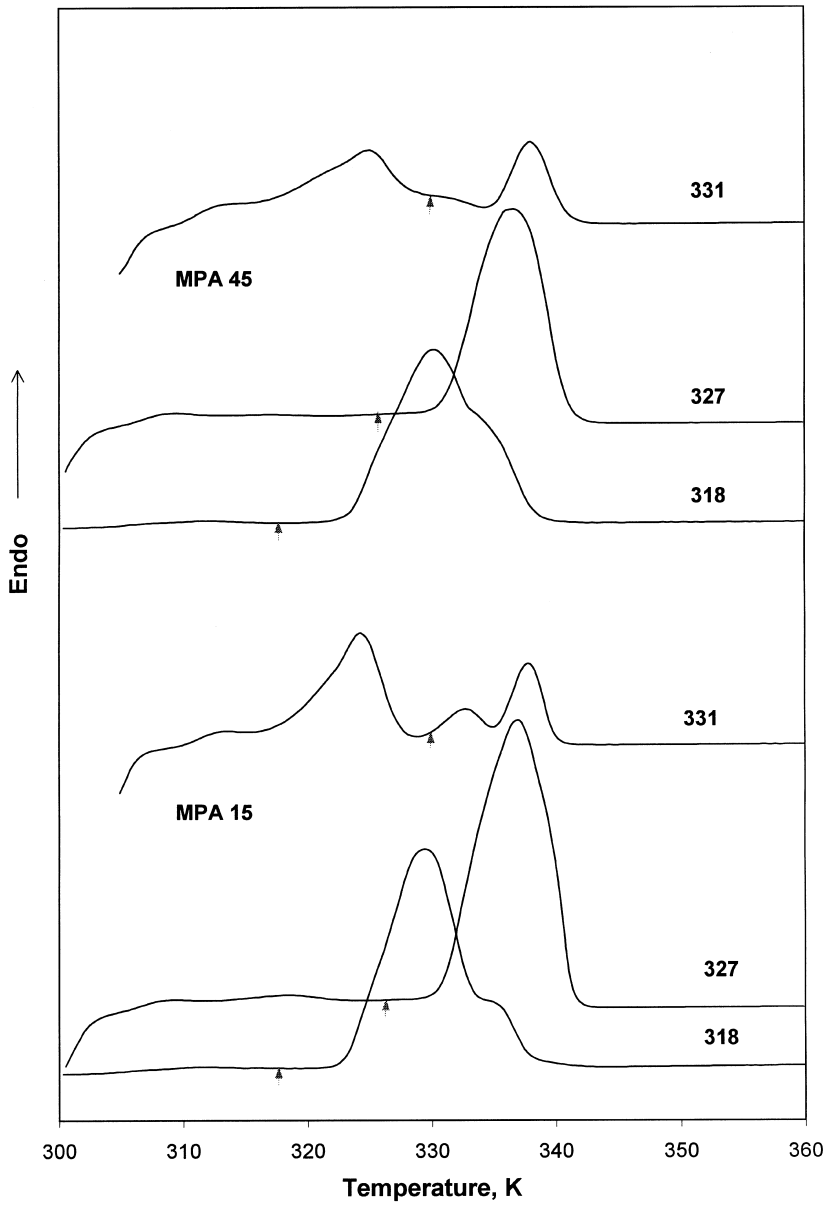

Fig. 2. The DSC thermograms of MPA 15 and MPA 45 annealed at indicated temperatures T_a (K) for 20 min, cooled (CR = −10 K/min) to 300 K and scanned (CR = −10 K/min). The arrows indicate respective T_a.

however, serve as a first approximation in looking for the recrystallization optimum of MPA. Fig. 4 shows the heats of fusion corresponding to structures III and IV in dependence on annealing temperature T_a. The dependence for ΔH_{IV} passes through a flat maximum at 327 K which might hence be considered a temperature optimum of MPA recrystallization. But, structure IV melts at about 335 K, i.e. above the range of annealing temperatures. Consequently, endotherms IV in the thermograms of Fig. 1 include in fact two contributions—structure IV formed during annealing at the respective T_a and structure IV formed by recrystallization during the subsequent DSC scan. Therefore, a better "inverse" measure of the degree of recrystallization could be the value of ΔH_{III} (or $\Delta H_{III} + \Delta H_{II}$ for $T_a = 331$ K) representing a portion of less-perfect crystallites remaining in the system after annealing at the respective temperature. It can be seen that the recrystallization optimum of MPA lies in the range of 327–329 K.

Fig. 5(A)–(C) presents thermograms of the three as-prepared MPA samples annealed at 327 K for 20 min. One can see that in all the three cases recrystallization reaches a similar high degree of conversion. The crystallites have been transformed into the final ordered structure IV characterized by T_m of about 336 K. Still, particularly in the case of MPA 5 (thermogram A), small endotherms are visible at about 310 and 320 K, apparently corresponding to the "fringed" lamellae I and II. From the thermograms B and C it can be seen that even though the recrystallization is a

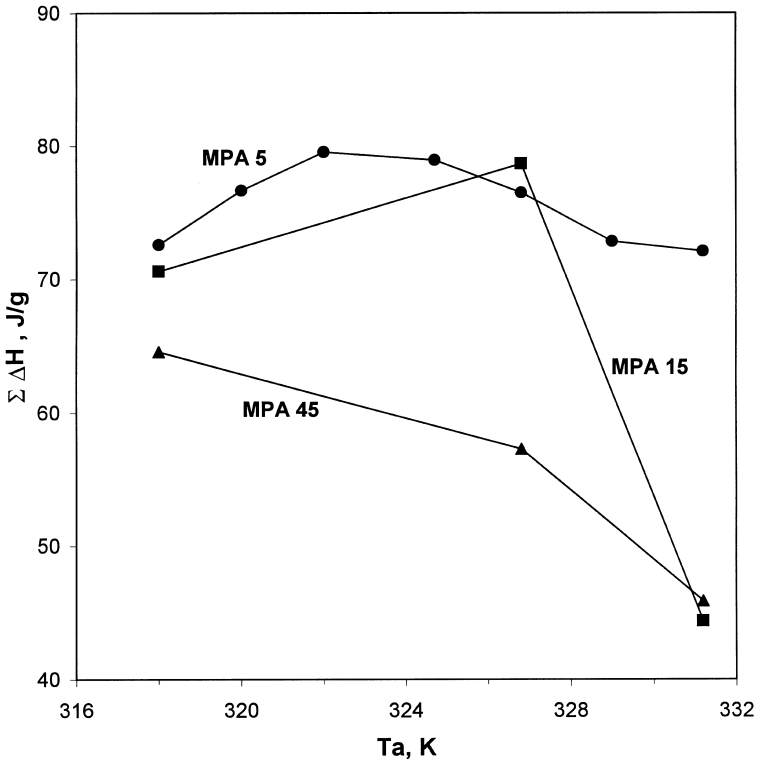

Fig. 3. The overall enthalpic balance of the DSC thermograms of MPA samples annealed at respective T_a (see Figs. 1 and 2).

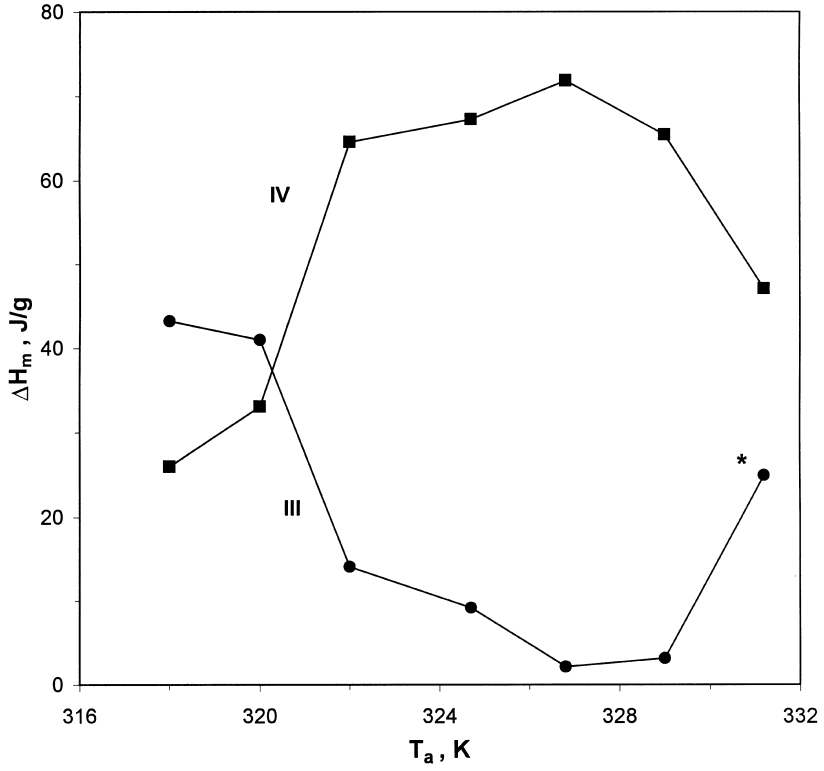

Fig. 4. The dependence of the heats of fusion of MPA 5 endotherms III and IV on annealing temperature T_a.

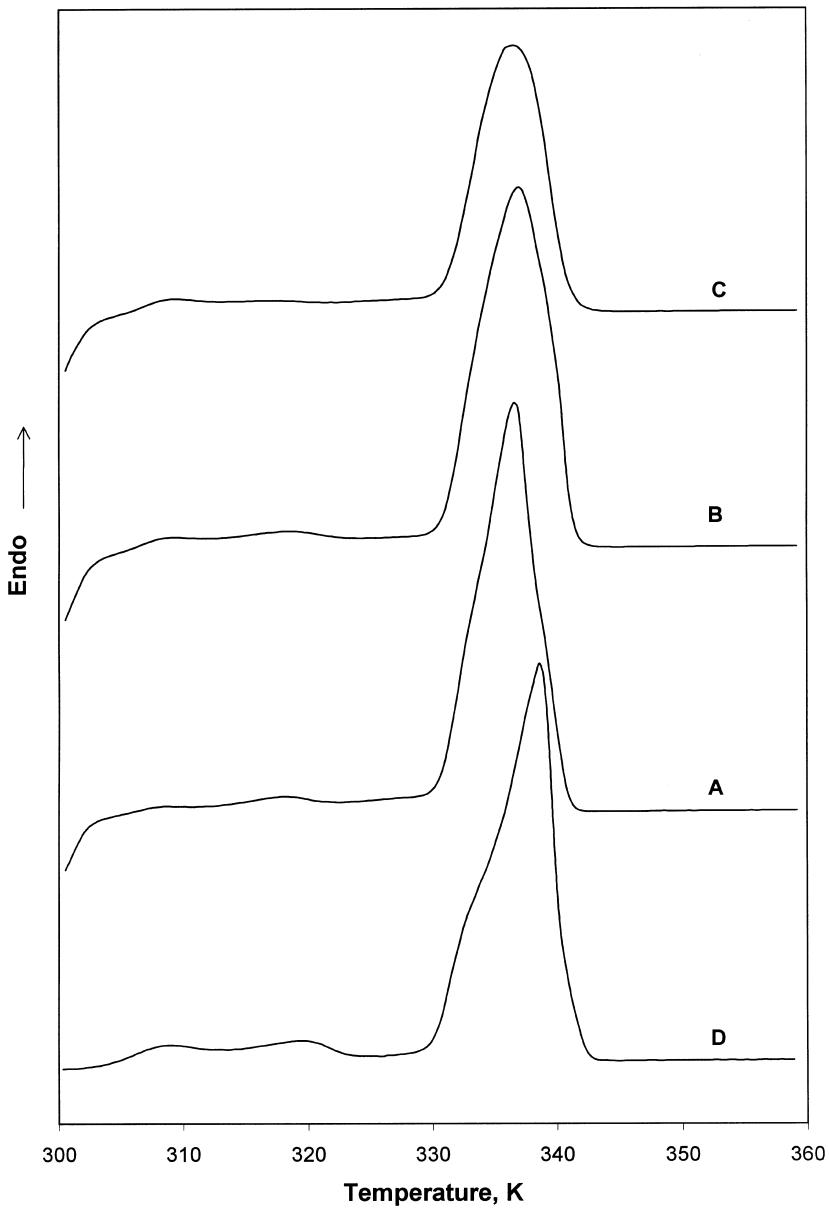

Fig. 5. The DSC thermograms of recrystallized MPA samples: (A) MPA 5; (B) MPA 15; (C) MPA 45 annealed at 327 K for 20 min; (D) MPA 5 annealed at 327 K for 20 min and left standing at laboratory temperature for 18 h.

diffusion-controlled and, consequently, a molecular-weight-dependent kinetic process, samples of different molecular weights reach the same degree of perfection of the final crystalline structure provided that they have been left at the optimum recrystallization temperature for a certain period of time.

The recrystallization process was also investigated from the viewpoint of possible time stability of the final recrystallized structure IV. Thermogram D in Fig. 5 corresponds to the MPA 5 sample that, after recrystallization at 327 K for 20 min, was left to relax at laboratory temperature for another 18 h and then scanned on DSC. The area of the main peak did not change but the endotherms corresponding to structures I and II were enlarged which indicates additional crystallization of the "fringed" lamellae during standing at laboratory temperature.

The maximum of the main peak in thermogram D is shifted towards higher temperatures which might imply a further perfection of the recrystallized ordered structure with the time of relaxation at laboratory temperature. By comparing the temperature maxima of MPA 5 endotherms IV in Fig. 5(A) and (D) with those of endotherms IV in Fig. 9 of the first part [1], one can easily detect a positive shift of the melting temperature of the annealed samples. Apparently, during the 20-min annealing at the optimum recrystallization temperature, the chains can reorganize to form a crystalline structure, which is more perfect than that formed by recrystallization during the DSC scan. A further

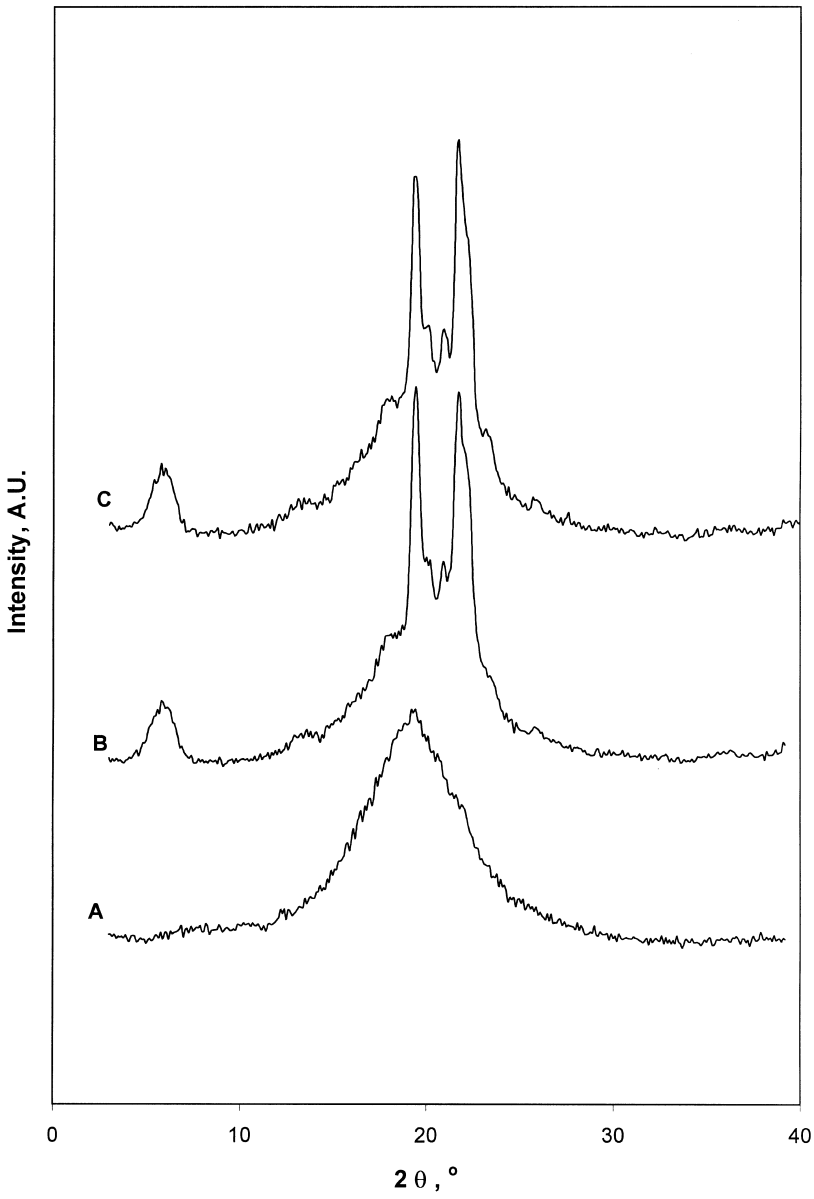

Fig. 6. The WAXS patterns of MPA 15 samples: (A) melted at 360 K, quenched; (B) as prepared; (C) recrystallized at 327 K, 20 min.

perfection of the crystalline structure takes place when the annealed sample is left to relax at laboratory temperature for a period of time (Fig. 5(D)).

A somewhat different interpretation of the DSC thermogram of poly(*N*-methyldodecano-12-lactam) was described by Shalaby et al. [2–4]. Their as-prepared sample of MPA showed a major endotherm at 327 K and a minor endotherm at 321 K. The sample that was melted, deep-quenched and then reheated showed two crystallization exotherms at 273 and 309 K and two melting endotherms at 299 and 326 K. The authors did not reveal any recrystallization behaviour which, based on our findings, is a characteristic feature of MPA. Two possible factors could be in play in this apparent discrepancy. The first is the effect of molecular weight. From the reduced viscosity data of Shalaby we have roughly estimated M_w at 80 000 which is a value considerably higher than that of our highest-molecular-weight sample, MPA 45 (see Table 1 in the first part [1]). As it has already been shown, molecular weight has a substantial impact on the recrystallization behaviour of MPA. The other reason for the absence of the recrystallization behaviour of MPA in the previous studies [2–4] can be attributed to the heating rate in the DSC scans. The value 20 K/min used by Shalaby et al. is quite a high scanning rate for the high-molecular-weight MPA system to undergo a complete recrystallization. The authors also mentioned that during scanning at a slower heating rate, the higher endotherm splitted into a doublet of major and minor components at 319 and 329 K. This might be attributed to a partial recrystallization, but the authors gave no details or comments.

The WAXS curves of the as-prepared, amorphous and recrystallized (20 min at 327 K) samples of MPA 15 are

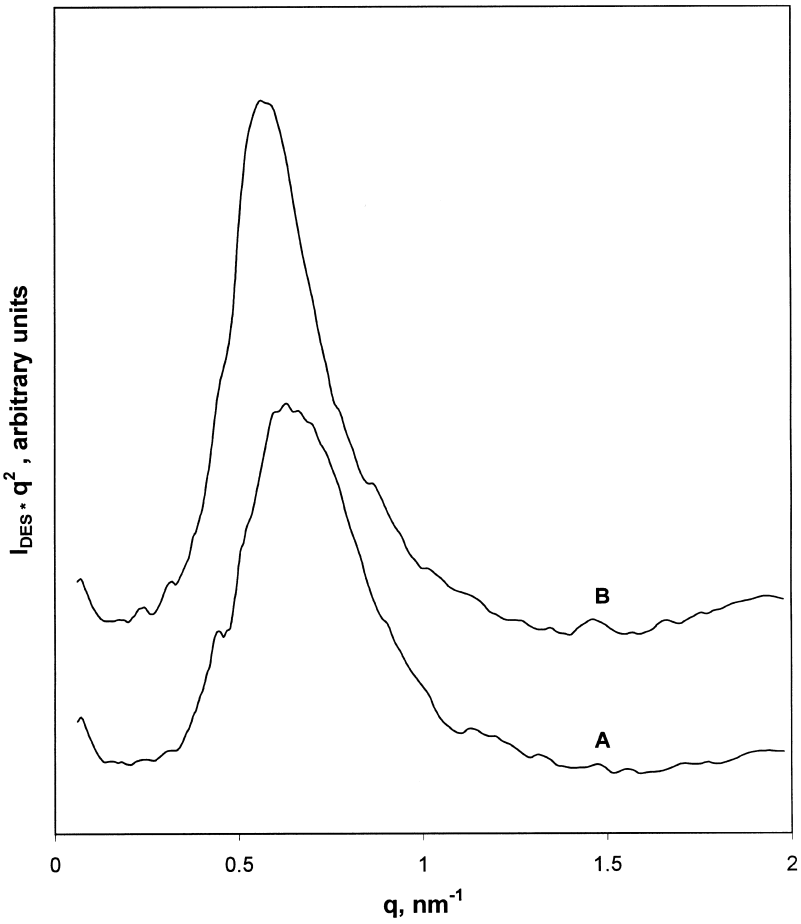

Fig. 7. The SAXS curves (intensity-desmeared and Lorentz-corrected in arbitrary units) of MPA 15: (A) as prepared; (B) recrystallized at 327 K, 20 min. q-scattering vector (see text for details).

presented in Fig. 6. The WAXS analysis has revealed that no change in crystalline modification takes place during the recrystallization process. Crystallinity increases to 35% during recrystallization as compared with 30% crystallinity of the as-prepared sample.

Fig. 7 gives the SAXS patterns of the MPA 15 sample. These curves show a maximum corresponding to the existence of periodicity in lamellar crystalline structure. While the crystalline modification of MPA does not change during recrystallization at 327 K, LP increases from the value of 10.0 nm for the as-prepared sample to 11.2 nm for the recrystallized sample.

Raman spectra of the isothermally crystallized (at room temperature) and subsequently recrystallized (at 327 K) MPA 15 samples are compared in Fig. 8. It can be seen that the main features of the spectra are identical, which indicates that the basic crystalline structure of both forms is the same, in agreement with the WAXS analysis. The degree of crystallinity of the recrystallized sample is slightly higher compared with the original isothermally crystallized sample. If the crystallinity is determined by using the intensity of the amorphous carbonyl band at 1643 cm^{-1}, its value increases from 42 to 48%.

Degrees of crystallinity obtained from the Raman carbonyl band are systematically higher compared with the data from WAXS. To get more insight into this observation, we have analyzed the other two frequency ranges in the Raman spectra of MPA sensitive to the transition from the amorphous to the crystalline phase, assigned [12] to the CH_2 twisting vibrations (centered around 1303 cm^{-1}) and C–C stretching vibrations (1050–1110 cm^{-1}) (Fig. 8). Using the results of thorough spectroscopic analyses of polyethylene and *n*-alkanes [13,14], the sharp peak at 1297 cm^{-1} and the doublet at 1106 and 1064 cm^{-1} can be correlated with the CH_2 sequences having all-*trans* conformation. The bands at 1305 and 1079 cm^{-1} correspond to disordered CH_2 sequences. Since the integral intensity in the CH_2 twisting range is independent of the chain conformation, it can serve as an internal standard [13,14]. It can be seen in Fig. 8 that, while the characteristic amorphous bands at 1643 and 1079 cm^{-1} are well compensated in the difference spectra C and F, the band at 1297 cm^{-1} assigned to the CH_2 twisting vibration is still asymmetric with a shoulder at 1305 cm^{-1}. The asymmetry can be removed when the subtracting factor f is increased as indicated in Fig. 8 (spectra D and G). The corresponding degrees of crystallinity for the

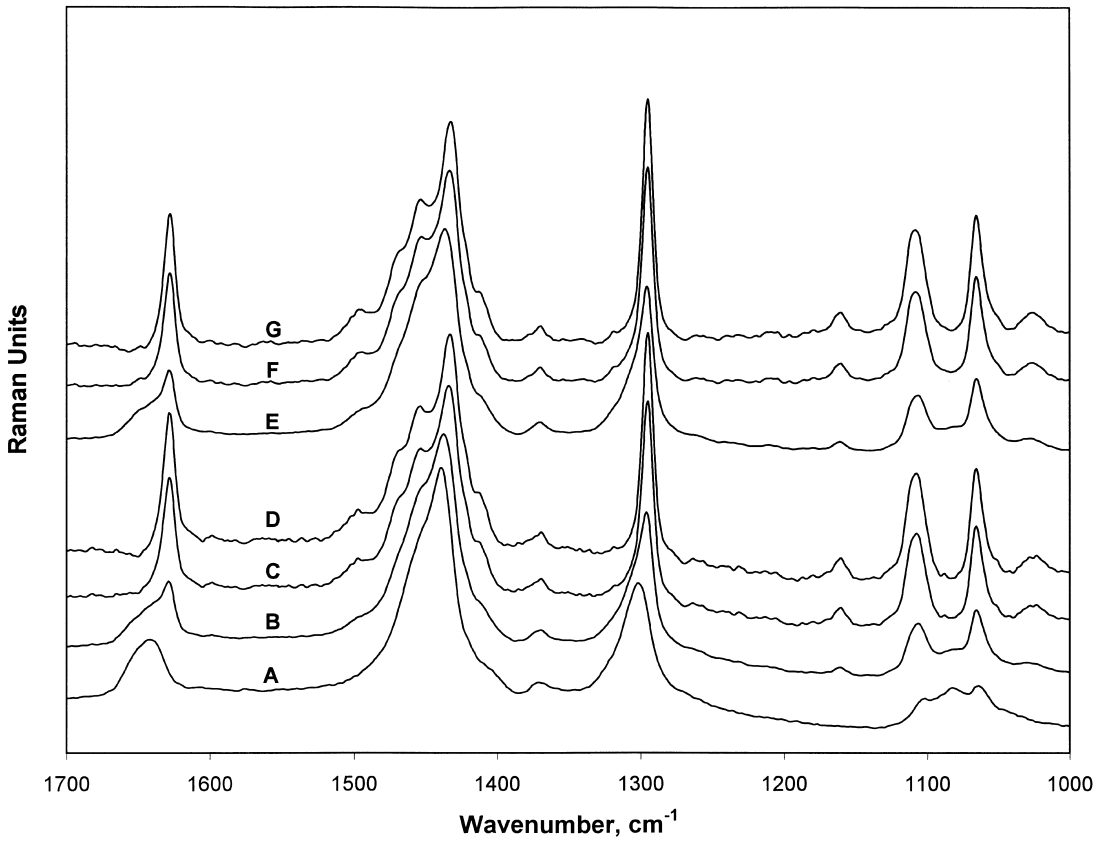

Fig. 8. The Raman spectra of MPA15: (A) amorphous, measured at room temperature immediately after cooling the melted sample (at 360 K for 10 min); (B) isothermally crystallized at room temperature for 48 h; (C) and (D) difference spectra B—$f\times$ A with the subtracting factor $f = 0.58$ and 0.75, respectively; (E) recrystallized by annealing at 327 K for 20 min and left standing at room temperature for 18 h; (F) and (G) difference spectra E—$f\times$ A with the factor $f = 0.52$ and 0.68, respectively.

room-temperature crystallized and recrystallized samples are 25 and 32%, respectively; these values are close to the WAXS data. We assume that the differences between the crystallinity assessed from the Raman spectra using the "amorphous" bands at 1643 and 1305 cm^{-1} follow from the existence of the interfacial region between the crystalline and amorphous phases characterized by partial ordering of the chain units. Such a third phase was clearly demonstrated in polyethylene [13,14] and recently also in polycarbonate [15].

In addition to the increase in the degree of crystallinity, the Raman spectra of the neat crystalline phase in the room-temperature crystallized and recrystallized samples differ also in the shape of the overlapping doublet at 1106 and 1111 cm^{-1} (see Fig. 9). The band is assigned to C–C stretching vibrations in the all-*trans* CH_2 sequences. The splitting is more pronounced in the spectrum of the recrystallized sample and it is probably caused by the vibrational coupling of the C–C stretching modes in the CH_2 sequences with exactly regular all-*trans* conformational structures. The regularity is characteristic of the recrystallized structures compared with slightly distorted CH_2 sequences appearing in the isothermally crystallized sample. It can be related to the change in the long period during recrystallization of MPA as follows from the SAXS measurements.

3.2. Different cooling rates

The influence of different cooling rates (CR) of melted samples on the crystallization process of MPA was studied in the range of CR from −1.25 to −320 K/min. The two extreme thermograms of MPA 5 are shown in Fig. 10(A) and (D). At a CR of −1.25 K/min (Fig. 10(A)) the first endotherm I is somewhat broader and is shifted to higher temperatures (about 265 K) as compared with the thermogram of the sample isothermally crystallized at $T_c = 250$ K [1]. This is probably associated with a higher degree of ordering of the "fringed" lamellae formed in the later stages of non-isothermal crystallization during slow cooling. Abrupt additional crystallization is demonstrated by a sharp exotherm E II with the minimum at 300 K. Subsequently, the system passes through the usual steps of melting of the ordered structure III, recrystallization (E III), and melting of the final crystalline structure associated with the narrow endotherm IV at about 334 K.

The character of the thermogram of the MPA 5 sample cooled at a CR of −320 K/min (Fig. 10(D)) is quite

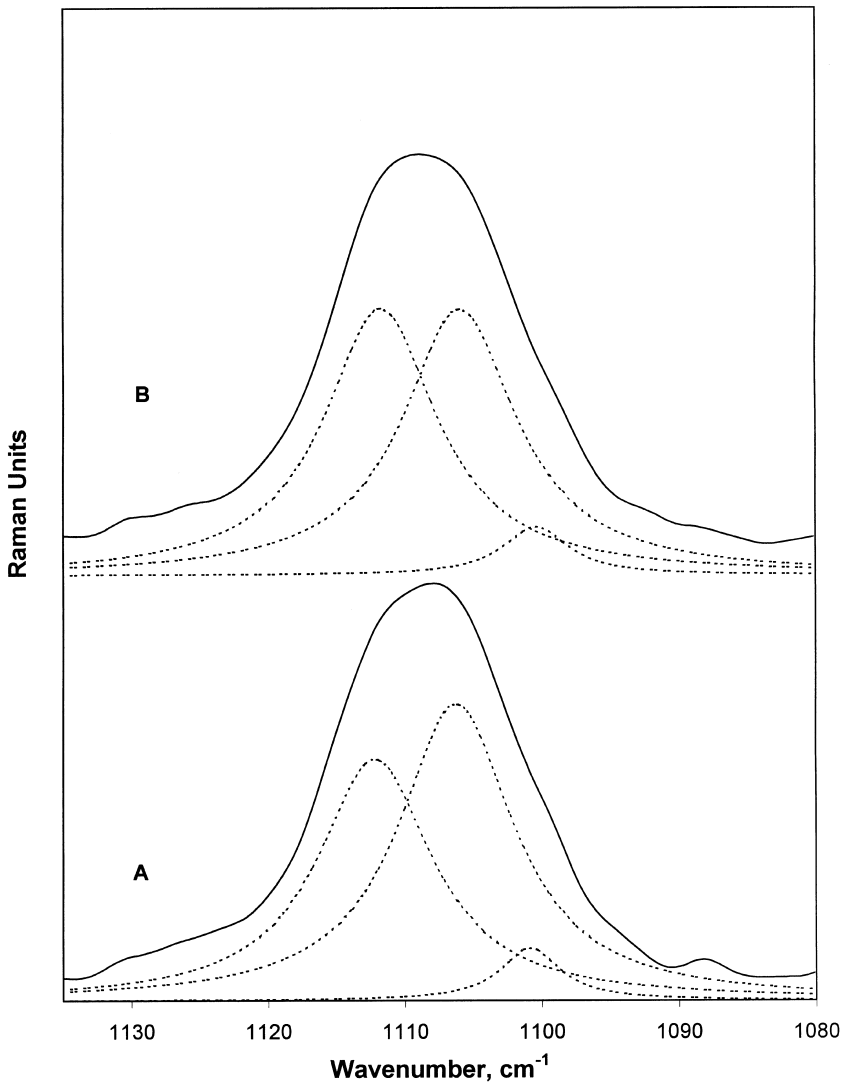

Fig. 9. The Raman spectra of MPA 15: (A) crystallized at room temperature; (B) recrystallized at 327 K. The spectrum of the amorphous component is subtracted (factor $f = 0.75$ and 0.68, respectively).

different. After the glass transition at about 240 K, the thermogram begins with a broad exotherm E I showing a minimum at 255 K. This exotherm is apparently associated with the relaxation of polymer chains after the shock supercooling of the system to a temperature below T_g and with the concomitant non-isothermal crystallization. This exotherm also overlaps the melting endotherm of the "fringed" lamellae which should otherwise appear in this temperature range and which is expressed here by a hump at 270 K only. Also the remaining part of the thermogram D is markedly influenced by the shock supercooling—a broader exotherm E II of additional crystallization, lower endotherms of the less-ordered and final crystalline structures III and IV, and a less pronounced recrystallization exotherm E III appear. Moreover, the maxima/minima of these endotherms/exotherms are shifted towards lower temperatures as compared with the corresponding peaks in the sample cooled at a CR of −1.25 K/min (Fig. 10(A)).

Thermograms B and C in Fig. 10 relate to the samples of MPA 15 and MPA 45, respectively, cooled at a CR of −1.25 K/min. One could contemplate that an increased molecular weight has, to a certain extent, a similar effect on the crystallization process of MPA as rapid supercooling. This is quite understandable if we consider that the crystallization processes taking place in the MPA samples before and during the DSC scans are diffusion-controlled and, consequently, significantly influenced by molecular weight and the speed of temperature changes.

3.3. Molecular interpretation of observed phenomena

Shalaby et al. [4] have shown that in the crystallization process of MPA a substantial role is played by the transition between *anti* and *syn* conformations of the amide group. They assume an equilibrium ratio of both conformations in the system with the crystalline phase containing chains

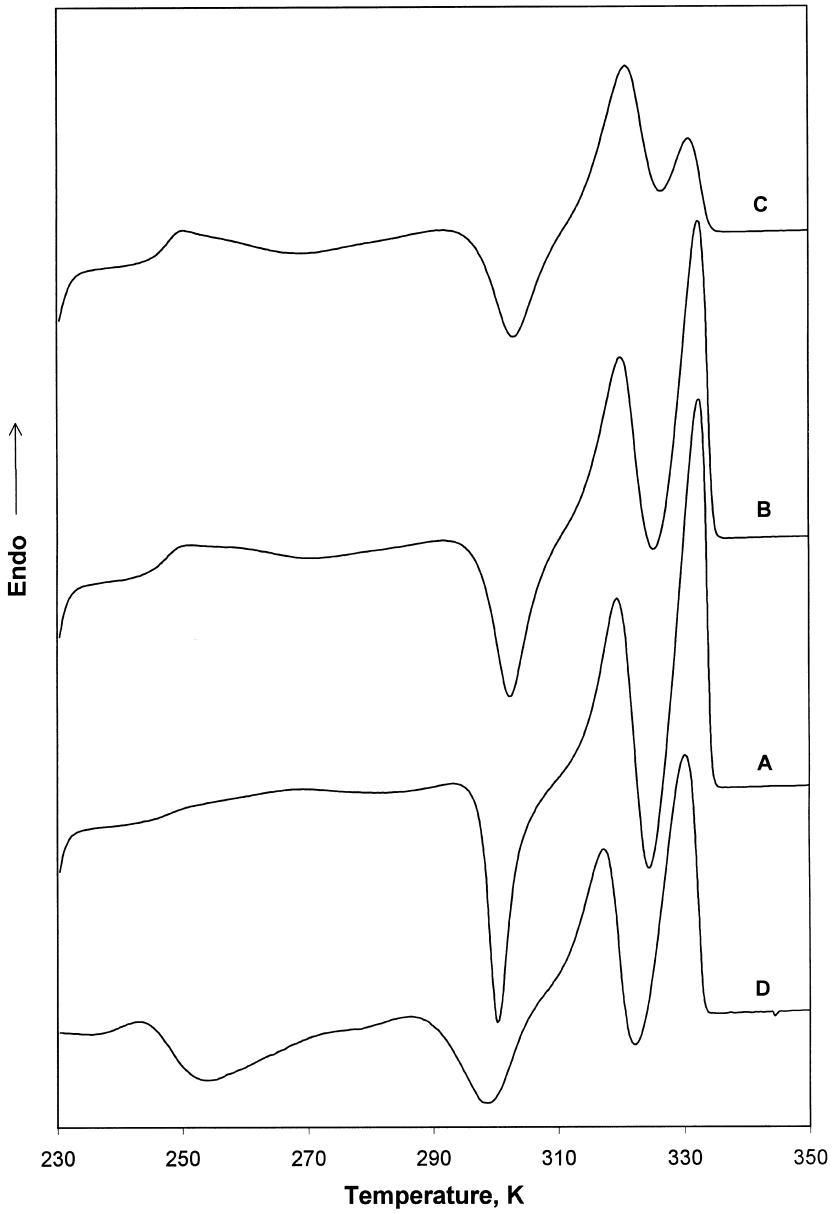

Fig. 10. The DSC thermograms of MPA samples after melting (360 K, 10 min) and cooling to 230 K at different rates CR: (A) MPA 5; (B) MPA 15; (C) MPA 45 cooled at CR = −1.25 K/min; (D) MPA 5 cooled at CR = −320 K/min.

with *anti* conformations on the amide group. Schmidt et al. [16] have shown by IR measurements that in amorphous MPA an equilibrium exists between *cis* and *trans* conformers on the amide group but that *cis* conformation is preferred in the crystalline phase of MPA. Our discussion below is based on these more recent findings.

During cooling from the melt, MPA chains or their parts containing *cis* amide conformers form the primary crystalline lamellae III. The *trans* conformers concentrate in the amorphous phase and, at temperatures lower than about 290 K, slowly relax from *trans* to *cis* conformation. This process facilitates the formation of "fringed" lamellae (I and II). At about 300 K a co-operative *trans*/*cis* transition takes place in MPA chains which is accompanied by additional crystallization of structure III associated with the appearance of pronounced exotherm E II on the DSC thermograms.

It follows from the above presented Raman spectroscopy results that the crystalline forms III and IV differ in the contents of *trans* and *gauche* sequences in the hydrocarbon parts of the MPA chains. Consequently, the defects leading to the lower melting temperature of form III can be attributed to the presence of the *gauche* C–C conformations. At about 327 K, the *gauche* conformers undergo a co-operative transition to the all-*trans* zig-zag arrangement of the CH_2 sequences. The lamellar structure IV thus formed is

characterized by a higher degree of crystallinity, higher melting temperature and higher value of the long period as compared with form III.

On the basis of the above discussed findings, the following possible mechanism of the complex crystallization/melting processes taking place in MPA can be proposed. On the molecular level, two conformational transitions have a fundamental influence on the crystallization behaviour of this polymer: *trans*/*cis* transition on the C–N bond and *gauche*/*trans* transition of the C–C sequences.

If we cool the system from the melt, an equilibrium is established between *cis* and *trans* conformations on the C–N bond. The chains containing *cis* C–N conformations can form the crystalline phase. Structure III (melting endotherm at about 324 K) is formed as primary lamellae. The hydrocarbon sequences of this structure contain defects caused by the *gauche* C–C conformations. After a relatively fast isothermal crystallization of form III and "spending" the chains with *cis* C–N conformers, a slow relaxation of the *trans* to *cis* C–N conformations proceeds in the amorphous phase. This transition facilitates the formation of the secondary "fringed" lamellae (form I and II). On heating, e.g. during the DSC scan, this relaxation on the C–N bond accelerates until, finally, at about 300 K a co-operative *trans*/*cis* transition on the C–N bond takes place which facilitates additional crystallization of form III associated with exotherm E II. During further heating, the number of defects in structure III caused by the *gauche* C–C conformations decreases until a cooperative transition takes place at about 327 K during which the all-*trans* C–C sequences are arranged in the MPA chains and the system recrystallizes (exotherm E III) to the final crystalline structure IV with the melting temperature at about 335 K. It might also be possible that the apparent existence of two types of "fringed" lamellae I and II has a reason similar to that of structures III and IV, i.e. different extents of the *gauche* C–C defects in the hydrocarbon sequences of the MPA chains.

4. Conclusions

Recrystallization during heating is a characteristic feature of poly(*N*-methyldodecano-12-lactam) MPA. In the DSC thermograms, it is associated with a recrystallization exotherm E III at about 326 K. During recrystallization, the primary crystalline structure III (melting at about 324 K) is transformed to a more perfect structure IV melting at about 335 K. The recrystallization process has proved to be irreversible and slowing down with increasing molecular weight. The optimum temperature of isothermal recrystallization of MPA is 327–329 K. After annealing at 327 K for 20 min, all three MPA samples show similar high degrees of recrystallization. After the same annealing process followed by relaxation at 300 K for 18 h, the resulting endotherm IV of MPA 5 shows a maximum at 338.8 K (65.6°C).

Crystallinity (WAXS) of MPA 15 increases from 30 to 35% during recrystallization with no change in the crystalline modification. The long period increases from 10.0 to 11.2 nm. Increase in crystallinity and no change in crystalline modification during recrystallization has also been proved by Raman spectroscopy. The spectra of the neat crystalline phase in the room-temperature crystallized and recrystallized samples differ in the shape of an overlapping doublet assigned to C–C stretching vibrations in all-*trans* CH_2 sequences. The splitting is more pronounced in the spectrum of the recrystallized sample and is attributed to vibrational coupling of the C–C stretching modes in the CH_2 sequences with exactly regular all-*trans* conformational structures.

The discrepancy in crystallinities assessed from Raman spectra and WAXS is apparently due to the spectroscopically detected interfacial region between the crystalline and amorphous phases characterized by partial ordering of chain units.

The DSC experiments with different cooling rates corroborate the idea that the crystallization/recrystallization of MPA is a diffusion-controlled kinetic process highly dependent on molecular weight and the rate of temperature changes.

On the molecular level, the crystallization/melting processes taking place in MPA can be interpreted as being directed by two conformational transitions in MPA molecules: the *trans*/*cis* transition on the C–N bond and the *gauche*/*trans* transition of the C–C sequences. After cooling from the melt, the primary structure III is formed predominantly from the chains containing *cis* C–N conformers. Subsequent slow *trans*/*cis* C–N relaxation facilitates the formation of interlamellar "fringed" crystallites. At about 300 K a co-operative *trans*/*cis* C–N transition facilitates additional crystallization of the primary lamellae III which contain a certain number of the *gauche* C–C defects. At about 327 K a co-operative transition takes place during which all-*trans* C–C sequences are arranged in crystallized MPA chains and the system recrystallizes to the final structure IV melting at about 335 K.

Acknowledgements

The authors would like to express their thanks to the Grant Agency of the Academy of Sciences of the Czech Republic (Grant No. A4050605) and the Grant Agency of the Czech Republic (Grant No. 203/97/0539) for financial support.

References

[1] Kratochvíl J, Sikora A, Baldrian J, Dybal J, Puffr R. Polymer 2000; 41:7653.
[2] Shalaby SW, Fredericks RJ, Pearce EM. J Polym Sci, Part A 1972; 10:1699.

[3] Shalaby SW, Fredericks R, Pearce EM. J Polym Sci Part B: Polym Phys 1973;11:939.
[4] Shalaby SW, Fredericks RJ, Pearce EM. J Polym Sci Part B: Polym Phys 1974;12:223.
[5] Ji XL, Zhang WJ, Wu ZW. J Polym Sci Part B: Polym Phys 1997; 35:431.
[6] Petrillo E, Russo R, D'Aniello C, Vittoria V. J Macromol Sci Phys B 1998;37:15.
[7] Wang S, Brisse F. Macromolecules 1998;31:2265.
[8] Kim HG, Robertson RE. J Polym Sci, Part B: Polym Phys 1998; 36:133.
[9] Cheng SZD, Zhang A, Barley JS, Chen J, Habenschuss A, Zschack PR. Macromolecules 1991;24:3937.
[10] Sarasua JR, Prud'homme RE, Wisniewski M, Le Borge A, Spassky N. Macromolecules 1998;31:3895.
[11] Puffr R, Tuzar Z, Mrkvičková L, Šebenda J. Makromol Chem 1983; 184:1957.
[12] Snyder RG. J Chem Phys 1967;47:1316.
[13] Strobl G, Hagedorn W. J Polym Sci Polym Phys Ed 1978;16:1181.
[14] Mutter R, Stille W, Strobl G. J Polym Sci Part B: Polym Phys 1993; 31:99.
[15] Dybal J, Schmidt P, Baldrian J, Kratochvíl J. Macromolecules 1998; 31:6611.
[16] Schmidt P, Straka J, Dybal J, Schneider B, Doskočilová D, Puffr R. Polymer 1995;36:4011.